DETERMINATION OF IMPACT PARAMETERS IN ALIGNED BREAKUP OF PROJECTILE-LIKE FRAGMENTS IN ^{197}Au + ^{197}Au COLLISIONS AT 23A MeV*

T. Cap[a,b], K. Siwek-Wilczyńska[b], J. Wilczyński[a†], F. Amorini[c,d]
L. Auditore[e], G. Cardella[f], E. De Filippo[f], E. Geraci[d,f]
L. Grassi[d,f], A. Grzeszczuk[g], E. La Guidara[f], J. Han[c], T. Kozik[h]
G. Lanzalone[c,i], I. Lombardo[j], R. Najman[h], N.G. Nicolis[k]
A. Pagano[f], M. Papa[f], E. Piasecki[l,a], S. Pirrone[f], R. Płaneta[h]
G. Politi[d,f], F. Rizzo[c,d], P. Russotto[f], I. Skwira-Chalot[b]
A. Trifiró[e], M. Trimarchi[e], G. Verde[f], W. Zipper[g]

[a]National Centre for Nuclear Research, Otwock/Warszawa, Poland
[b]Faculty of Physics, University of Warsaw, Warszawa, Poland
[c]INFN, Laboratori Nazionali del Sud, Catania, Italy
[d]Dipartimento di Fisica e Astronomia, Università di Catania, Catania, Italy
[e]Dipartimento di Fisica, Università di Messina
and INFN Gruppo Collegato di Messina, Messina, Italy
[f]INFN, Sezione di Catania, Catania, Italy
[g]Institute of Physics, University of Silesia, Katowice, Poland
[h]The M. Smoluchowski Institute of Physics, Jagiellonian University
Kraków, Poland
[i]Università Kore, Enna, Italy
[j]Dipartimento di Fisica, Università di Napoli and INFN — Sezione di Napoli
Napoli, Italy
[k]Department of Physics, University of Ioannina, Ioannina, Greece
[l]Heavy Ion Laboratory, University of Warsaw, Warszawa, Poland

(Received January 18, 2016)

Symmetric and asymmetric aligned breakup of projectile-like fragments in ^{197}Au + ^{197}Au collisions at 23A MeV was studied. Independently of the asymmetry, the reaction yields have been found peaked at a common, very narrow range of impact parameters.

DOI:10.5506/APhysPolB.47.983

* Presented at the XXXIV Mazurian Lakes Conference on Physics, Piaski, Poland, September 6–13, 2015.

† Deceased.

1. Introduction

Collisions of very heavy nuclear systems, such as ^{197}Au+^{197}Au, attract the interest of researchers mostly because of the complete elimination of fusion processes which cannot occur due to the Coulomb instability of such super-heavy composite systems. Consequently, a wide range of impact parameters corresponding to semi-peripheral and near-central collisions is open to fast dynamical rearrangements of nuclear matter and new exotic processes.

Ternary breakup of heavy nuclear systems [1–3] proceeds as a rule sequentially, in two stages. In the first stage, a large portion of kinetic energy is dissipated and an excited projectile-like fragment (PLF*) and excited target-like fragment (TLF*) are formed as a result of the exchange of many nucleons between the target and projectile

$$^{197}\mathrm{Au} + {}^{197}\mathrm{Au} \rightarrow \mathrm{TLF}^* + \mathrm{PLF}^* \,. \tag{1}$$

In the second stage of the reaction, either the PLF* or TLF* breaks up. In the case of an initially symmetric system, both decay modes are identical, so it is enough to study half of the events in which the PLF* breaks up into fragments F1 and F2

$$\mathrm{PLF}^* \rightarrow \mathrm{F1} + \mathrm{F2} + \text{evaporated light particles} \,. \tag{2}$$

In our notation, F1 denotes the *heavier* fragment of mass number A_{F1} and F2 denotes the *lighter* one of mass number A_{F2}.

2. Experiment

The experiment was performed at the INFN Laboratori Nazionali del Sud (LNS) in Catania, Italy. A beam of ^{197}Au ions from the LNS Superconducting Cyclotron was accelerated to an energy of 23A MeV and bombarded a ^{197}Au target placed inside the Charged Heavy Ion Mass and Energy Resolving Array (CHIMERA) [4]. The CHIMERA multidetector is arranged in 4π geometry and is built of 1192 two-layer ΔE–E telescopes, each consisting of a planar 275 μm-silicon detector and a CsI(Tl) scintillator. Detailed information on methods of mass identification and fragment energy determination with the CHIMERA detection system is given in [5].

3. Reconstruction of *cold* projectile-like fragments (PLF) and *hot* (PLF*) fragments

Figure 1 shows the mass number distribution of pairs of fragments F1 and F2 formed in the process described by Eq. (2). The distributions are

plotted as a function of the ratio $f = A_{F2}/(A_{F1} + A_{F2})$ which is a measure of asymmetry of the breakup. Only pairs of fragments for which both A_{F1} and A_{F2} are greater than 7 and $A_{F1} + A_{F2} \geq 160$ are taken into account in the analysis. One can see from Fig. 1 that pairs of fragments F1 and F2 of all possible asymmetries are produced. Especially intensively populated is a group of very asymmetric partitions corresponding to $f \leq 0.1$. Characteristics of typical "intermediate mass fragments" (IMF) (of mass numbers up to 20), observed in other experiments at low [7, 8] and higher energies [9–12] fit these asymmetric partitions. However, apart from pairs involving IMFs, more symmetric divisions are also observed in our experiment. In the following part of this paper, we will concentrate only on partitions corresponding to $f > 0.1$.

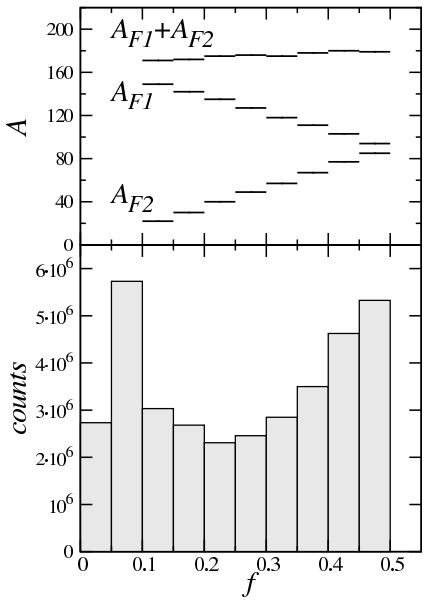

Fig. 1. Distribution of asymmetry parameter (lower panel). Average mass numbers of fragments F1, F2 and their sum (upper panel). For more details, see Table I.

Initially, we analyze our data in a simplified approach neglecting the influence of evaporated light particles (see Eq. (2)) in the balance of momenta. Thus, the reaction is studied by viewing the velocity vectors of *cold* (de-excited) fragments ($\vec{v}_{F1}$, $\vec{v}_{F2}$) and *cold* PLF ($\vec{v}_{PLF}$) defined in the center-of-mass reference frame of the ^{197}Au+^{197}Au system. Here, the vector $\vec{v}_{PLF}$ is the velocity of the center-of-mass of the F1+F2 subsystem (reconstructed PLF).

The correlations between the total kinetic energy (TKE) and center-of-mass emission angle $\Theta_{\mathrm{C.M.}}$ for reconstructed *cold* PLFs are shown in Fig. 2 for three selected bins of the asymmetry parameter f (TKE is calculated as

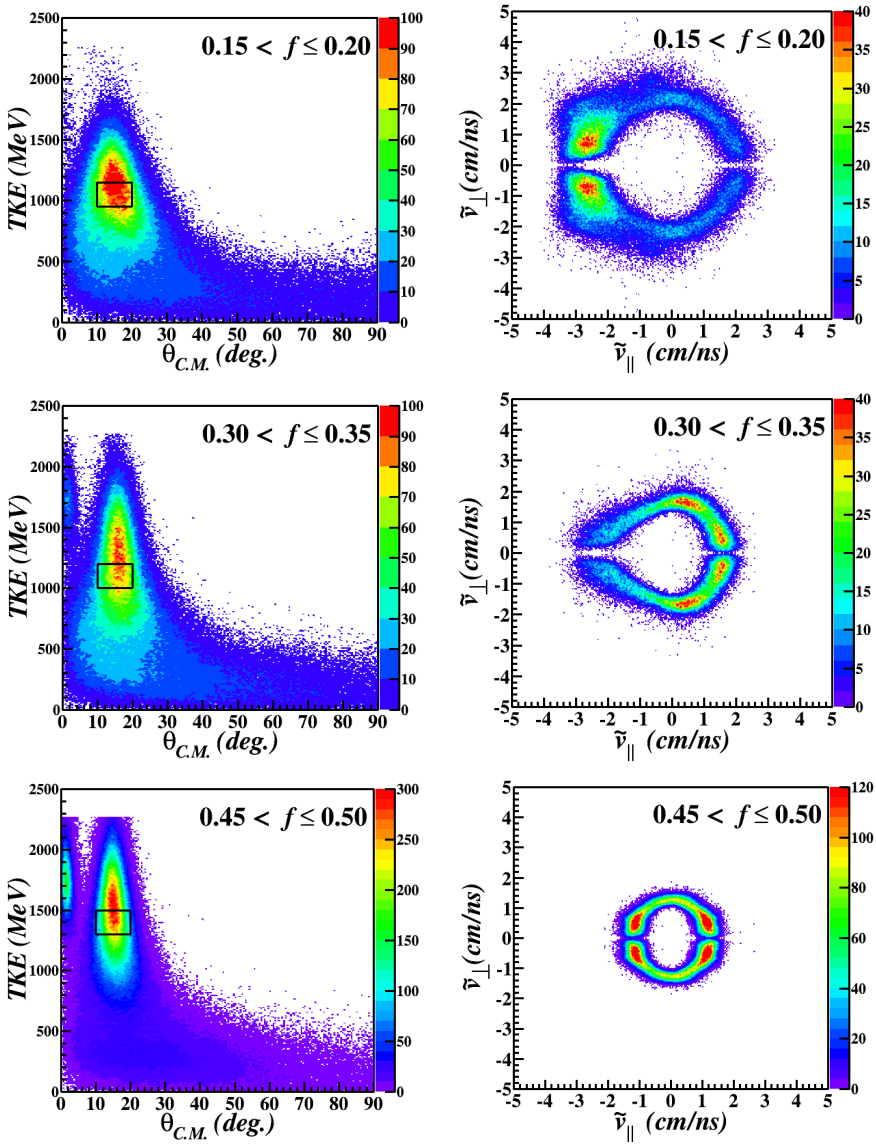

Fig. 2. TKE *vs.* $\Theta_{\mathrm{C.M.}}$ diagrams of *cold* PLFs for three selected asymmetries (left column) and velocity distributions of lighter fragments F2 in the PLF systems (right column) evidently demonstrating Coulomb rings for events located within the limiting rectangular gates.

the sum of kinetic energies of the *cold* PLF and complementary *cold* TLF calculated from momentum balance when the momenta of evaporated nucleons are neglected). One can see in Fig. 2 that, independently of the asymmetry of the breakup, the most probable events are localized in a rather narrow range of the PLF deflection angles $\Theta_{\mathrm{C.M.}} \approx 15^\circ$ and in a well-defined range of total kinetic energy corresponding to a considerable but not complete loss of kinetic energy.

Next, we studied the decay of the projectile-like fragments into F1 and F2. This was done in the reference frame fixed to the center of mass of the reconstructed PLF, with one coordinate directed along the TLF*–PLF* separation axis [6]. In the right column of Fig. 2, we display velocity distributions in this reference frame by plotting the transverse component $\tilde{v}_\perp$ *vs.* the longitudinal component $\tilde{v}_\parallel$ of the velocity of the *lighter* fragment (F2). Events are clearly distributed on rings, a fact that demonstrates an approximately constant value of relative velocity in the F1+F2 subsystem. In fact, the observed rings exactly correspond to the value of relative velocity of pure Coulomb repulsion between fragments F1 and F2. The panel shown on top of the right column in Fig. 2 demonstrates that light fragments F2 are mostly emitted from the *neck* between the primary target-like fragment and the primary projectile-like fragment. However, for some more symmetric events ($f = 0.30$–0.35), a significant part of the light fragments F2 are seen on the opposite side, at forward angles. Detailed analysis of angular distributions requires corrections accounting for the detection efficiency of coinciding fragments. These effects have been studied separately but are not discussed in this work.

Some quantitative results of our analysis are collected in Table I. The first four columns show separately the asymmetry parameter bin width, the corresponding mass numbers A_{F2}, A_{F1} and A_{PLF} of the lighter fragment, heavier fragment and their sum, respectively. The fifth column shows the value of the total kinetic energy (TKE) of the *cold* PLF and complementary *cold* TLF. The results represent the most probable events located within the rectangular 200 MeV $\times$ 10 deg gates shown for a given asymmetry in Fig. 2.

We propose a simple method of calculating corrections which have to be applied to *cold* values of TKE converting them into the correct *hot* values TKE* (sum of kinetic energies of PLF* and TLF*). Assuming that the *average* velocity of all nucleons of the primary PLF* is not affected by the evaporation of nucleons from the PLF*, one can readily show that the ratio TKE*/TKE can be expressed as a function of the ratio $k = A_{\mathrm{PLF}^*}/A_{\mathrm{PLF}}$ of the mass numbers of the PLF* and PLF

$$\frac{\mathrm{TKE}^*}{\mathrm{TKE}} = \frac{k(A_{\mathrm{tot}} - A_{\mathrm{PLF}})}{A_{\mathrm{tot}} - kA_{\mathrm{PLF}}}\,, \tag{3}$$

TABLE I

Characteristics of breakup of Au-like primary fragments as a function of the breakup asymmetry parameter f. Numbers represent average values. The last three columns show the results of HICOL calculations (see the text).

f	A_{F2}	A_{F1}	A_{PLF}	TKE [MeV]	A_{PLF^*}	TKE* [MeV]	N_{trans}	L [$\hbar$]	J_{PLF^*} [$\hbar$]	N_{exch}
1	2	3	4	5	6	7	8	9	10	11
0.10–0.15	22	149	171	1150	196	1493	−1	1030	103	29
0.15–0.20	30	142	172	1050	201	1412	4	1003	98	34
0.20–0.25	40	135	175	950	207	1329	10	976	118	40
0.25–0.30	49	127	176	950	208	1330	11	976	118	40
0.30–0.35	57	118	175	1100	203	1458	6	1017	108	32
0.35–0.40	67	111	178	1300	199	1622	2	1066	88	25
0.40–0.45	77	103	180	1400	198	1699	1	1091	78	22
0.45–0.50	85	94	179	1400	198	1699	1	1091	78	22

where A_{tot} is the combined mass number of the colliding system. A value of the coefficient k can be approximately estimated assuming purely statistical emission of the missing nucleons. The whole system of mass number A_{tot} can emit N_{evap} nucleons, $N_{evap} = (E_0 - \mathrm{TKE}^*)/\epsilon$, where E_0 is the center-of-mass kinetic energy of the colliding system and ϵ is the average amount of excitation energy necessary to evaporate one nucleon. A reasonable value of this parameter is $\epsilon \approx 15$ MeV. The number of nucleons emitted from the primary PLF* fragment is equal to $A_{PLF^*} - A_{PLF} = (E_0 - \mathrm{TKE}^*)A_{PLF^*}/\epsilon A_{tot}$ (proportionality of the excitation energy to fragment masses is assumed). This leads to the relation

$$k = \frac{\epsilon A_{tot}}{\epsilon A_{tot} + \mathrm{TKE}^* - E_0} \tag{4}$$

with the unknown value of TKE*. One can calculate the coefficient k from a recurrence formula starting from the first order approximation, in which $\mathrm{TKE}^* = \mathrm{TKE}$ is assumed.

Calculated values of TKE* and estimated mass numbers of the primary fragments A_{PLF^*} for a given asymmetry parameter f are listed in Table I in columns seventh and sixth, respectively. Estimates of the resulting net transfer of nucleons in the primary stage of the reaction, $N_{trans} = A_{PLF^*} - 197$ are also given in Table I (the eighth column). One can see that differences between TKE and TKE* are significant and they must be accounted for in attempts to interpret theoretically the data.

4. Localization in angular momentum space

In order to obtain information on the localization of the PLF* breakup reactions in impact parameter/angular momentum space, we carried out calculations using the well-tested nuclear dynamics model HICOL of Feldmeier [13], based on the concept of multinucleon exchange, which predicts very strong energy dissipation. The theoretical dependence of the total kinetic energy TKE* on the angular momentum of relative motion L calculated for ^{197}Au+^{197}Au collisions at 23A MeV is shown in the left panel of Fig. 3. In the right-hand side panel, the combined amount of orbital angular momentum transferred to the PLF* and TLF* is shown. Provided the inertia of the colliding system is calculated in HICOL sufficiently realistically, the inelasticity of the reaction (*i.e.* the TKE* value) unambiguously determines the resulting localization of the reaction in L-space.

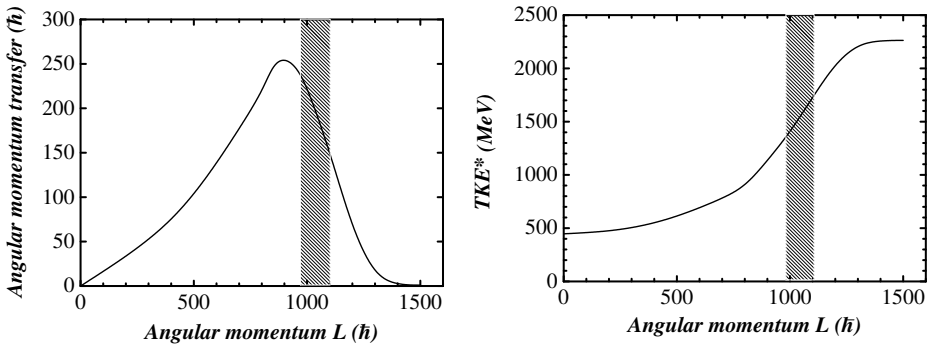

Fig. 3. Calculations with the code HICOL of the total kinetic energy TKE* and the angular momentum transfer for the ^{197}Au+^{197}Au reaction at 23A MeV. Dashed areas in both plots show the corresponding range for groups of events within the rectangular gates in Fig. 2.

The HICOL calculations have been done for all groups of experimental events shown in Fig. 2 (within the limiting rectangular gates). Surprisingly, independently of the asymmetry of the breakup, the reactions turned out to be localized in quite a narrow range of L-values, $L \approx 1000$–$1100\ \hbar$ (see also the ninth column in Table I). This corresponds to a very large but not complete damping of the available kinetic energy (the grazing trajectory angular momentum for these reactions is $L_{\rm graz} \approx 1570\ \hbar$).

The calculated angular momenta transferred to final PLF* and TLF* ($J_{\rm PLF^*}$, the tenth column in Table I) as well as the calculated number of nucleons exchanged between primary fragments ($N_{\rm exch}$, the eleventh column) are also of the highest interest because they may shed light on the nature of the dynamical disturbance causing breakup. A detailed analysis is under way.

This work was supported by the Polish National Science Centre under Contract No. UMO-2014/14/M/ST2/00738 (COPIN-INFN Collaboration).

REFERENCES

[1] I. Skwira-Chalot *et al.*, *Phys. Rev. Lett.* **101**, 262701 (2008).
[2] J. Wilczyński *et al.*, *Phys. Rev. C* **81**, 024605 (2010).
[3] J. Wilczyński *et al.*, *Phys. Rev. C* **81**, 067604 (2010).
[4] A. Pagano *et al.*, *Nucl. Phys. A* **734**, 504 (2004).
[5] T. Cap *et al.*, *Phys. Scr.* **T154**, 014007 (2013).
[6] T. Cap *et al.*, *Phys. Scr.* **89**, 054005 (2014).
[7] P. Glassel, D. von Harrach, H.J. Specht, *Z. Phys. A* **310**, 189 (1983).
[8] A.A. Stefanini *et al.*, *Z. Phys. A* **351**, 167 (1995).
[9] F. Bocage *et al.*, *Nucl. Phys. A* **676**, 391 (2000).
[10] E. De Filippo *et al.*, *Phys. Rev. C* **71**, 044602 (2005).
[11] E. De Filippo *et al.*, *Phys. Rev. C* **71**, 064604 (2005).
[12] J. Łukasik *et al.*, *Phys. Lett. B* **566**, 76 (2003).
[13] H. Feldmeier, *Rep. Prog. Phys.* **50**, 915 (1987).